Latin American Journal of Solids and Structures
www.lajss.org

Analysis of a tuned liquid column damper in non-linear structures subjected to seismic excitations

Abstract
The behavior of the tuned liquid column damper (TLCD) is analyzed in the control of non-linear structures subjected to random seismic excitations. The structure is modeled as a system of one degree of freedom with incursion in the non-linear range. The Bouc-Wen hysteretic model is used to model the non-linear behavior of the structure. A stationary stochastic analysis is performed in the domain of the frequency. An equivalent statistical linearization was used for the analysis of the main system and the TLCD. The TLCD parameters considered for the optimization process were the frequency and the head loss coefficient. Two target functions were considered, (i) reduction of the main displacement of the system, (ii) reduction of the hysteretic energy. Two random processes were considered as seismic excitation, first a broad bandwidth process and secondly a narrow bandwidth process. The results show that for a broad bandwidth process, the TLCD tends to tune with the linear equivalent frequency of the system in the case without TLCD, while for the narrow bandwidth process, it tunes (TLCD) with the dominant frequency of the input. It is seen that the TLCD becomes detuned with regard to the frequency of the structure as the structure becomes more non-linear. It is also seen that the optimal tuning ratio of the TLCD is unsensitive to the mass ratio of the device and the main damping ratio of the system. It is also concluded that in case of flexible structures, the optimal head loss coefficient tends to be lower and increases with regard to its length ratio. It is seen that the effectiveness of the TLCD is greater for higher mass ratios of the device. In addition, it is found that the optimal TLCD becomes less effective as the structure enters the non-linear range, showing lower efficiency than what is seen in the literature for optimal TLCDs in linear structures.

Keywords
Tuned liquid column damper, non-linear structures, hysteretic energy.

Gilda Espinoza[a]*
Carlos Carrillo[a]
Alvaro Suazo[a]

[a] Departamento de Ingeniería Civil y Ambiental, Universidad del Bío-Bío, Collao, Concepción. Chile. E-mail: gespinoz@ubiobio.cl, carcarri@alumnos.ubiobio.cl, asuazo@ubiobio.cl

*Corresponding author

http://dx.doi.org/10.1590/1679-78254845

Received: January 19, 2018
In Revised Form: April 26, 2018
Accepted: May 05, 2018
Available Online: May 10, 2018

1 INTRODUCTION

In order to provide functionality, serviceability and safety for the structures, new alternatives have arisen which allow to avoid the structural oversizing. Sakai & Takaeda (1989) introduces a device called tuned liquid column damper (TLCD), which consists of a "U" shaped container which contains liquid (typically water), which has an oscillation frequency and also has an orifice in the horizontal part of the tube which causes head loss. Xu et al. (1992) numerically show that with suitable parameters, the TLCD has an effectiveness that is similar to the tuned mass damper (TMD) in controlling the response of wind sensitive structures. Balendra et al. (1995) studied the effectiveness of the TLCD in the control of vibrations for towers with a broad range of natural frequencies, concluding that the performance of the TLCD does not solely depend on the tuning ratio but also on the opening ratio of the orifice. Battista et al. (2008) and Souza (2003) propose a hybrid fluid-dynamic control system (HTLCD) for active/passive control of bending oscillations of tall and slender buildings under wind forces. They conclude that when comparing uncontrolled and controlled responses of a tall and slender tower in terms of top horizontal displacement versus time and acceleration versus time, the HTLCD is more effective than two TLCD in orthogonal directions (DTLCD).

Given the advantages of the TLCD in terms of implementation, effectiveness and cost, further research has been made covering the potentiality of the TLCD in seismic engineering. Won et al. (1996) study the performance of the TLCD for the passive control of structures subjected to a non-stationary stochastic process with modulated

amplitude and frequency representing a strong earthquake. The study was made about the design parameters, like the mass ratio, head loss coefficient and tuning ratio, concluding that the design parameters depend on the frequency control, intensity and duration of the load applied.

Gao et al. (1997) obtain the optimal parameters of the TLCD for the maximum reduction of the response peak, for a variety of flexible structures subjected to a harmonic excitation in a wide range of frequencies. Gao et al. (1999) study the characteristics of Multiple Tuned Liquid Column Dampers (MTLCD) in the control of the structural vibration. It is concluded that an optimized MTLCD can be more effective than the traditional TLCD in reducing the structural response, and that the effectiveness of the MTLCD is sensitive to the amount of TLCD that is used, as long as there are five or less. Sadek et al. (1998) determine the design parameters of the TLCD and MTLCD under a seismic setting. They used 72 accelerograms to study the tuning, damping and length of the container in optimal TLCD, the central tuning ratio, and bandwidth tuning in the MTLCD. Yalla & Kareem (2000) obtain the optimal head loss coefficient, starting from a closed solution, based on the equivalent linearization and random vibration analysis, for an undamped system of one degree of freedom subject to a filtered white noise. The same analysis was extrapolated to MTLCD systems through a modal analysis (Yalla & Kareem, 2000), Shum (2009) develops a TLCD-closed solution structure outline, which allows obtaining optimal parameters of a TLCD. The TLCD-Structure interaction equations were derived and resolved both for the time and frequency domains.

Ghosh & Basu (2004) investigate the effectiveness of the TLCD in the control of short period structures subjected to seismic excitations. They use a model where the TLCD is connected by means of a spring to the main structure, removing the requirements over the natural period of the liquid of the TLCD. Lee et al. (2010) experimentally study the variation of the dynamic characteristics of the TLCD versus the excitations of different amplitude. They conclude that the natural frequency, damping factor and the ratio between the liquid mass and horizontal liquid mass affect the dynamic behavior of the TLCD. Chakraborty et al. (2012) perform a numeric study of the seismic performance of the TLCD, considering the effect of the restriction imposed on the maximum displacement of the liquid within the container.

Zeng et al. (2015) introduce an "S" shaped liquid damper to suppress the horizontal and vertical movement on floating oil platforms. Rozas et al. (2016) propose a bidirectional TLCD, which comprises two TLCDs placed orthogonally. This setup requires less water mass than two equivalent TLCDs. Di Matteo et al. (2015) provide a new oscillatory movement model of the liquid contained in the TLCD based on a fractional calculation mathematical tool. This model accurately describes the displacements of the surface of the liquid.

Bigdeli & Kim (2015) experimentally identify the inherent damping of three passive control devices: the TMD, tuned liquid damper (TLD) and TLCD, with regard to the damping effect of the mass that these constitute. For this, they use a steel three storey model subjected to dynamic excitation. They conclude that the device with the inherent damping that contributes more in the reduction of the energy is the TMD, followed by TLCD and finally, TLD. Cammelli & Li (2016) proposed TLCD as a solution for a 42-storey residential building which showed in its early design stage, displacements which would exceed the comfort criterion used in the industry.

Although there are numerous studies about the effectiveness of the TLCD, they mainly circumscribe to the analysis of linear systems. In fact, there is little on the performance of the TLCD in non-linear structures. Esteva & Ruiz (1997) conclude that the TLCD has two issues: first, that the reduction of the displacement is very sensitive to the tuning ratio, and second, when the frequency of the input is close to that of the main system, the reduction of the response reduces as it enters the non-linear range. Ghosh & Basu (2008) study the efficiency of a TLCD connected by means of a spring to a non-linear system with high initial rigidity, concluding that the reduction of the response is not considerable. However, the reduction of the structural response is not the only criterion to study the effectiveness of the TLCD; hysteric energy is also an excellent way to evaluate the dynamic behavior of a structure.

Finally, this investigation has the goal of analyzing the behavior of a TLCD in a structure with non-linear behavior and assessing its effectiveness in controlling the response of the structure in terms of the reduction in the displacement of the main system and the hysteretic energy dissipated

2 METHODOLOGY

2.1 STRUCTURAL MODEL

The structural model comprises a system of a damped one-degree-of-freedom structure with non-linear behavior modeled by the Bouc-Wen hysteretic element, having a tuned liquid column damper (TLCD) added, as can be seen in Figure 1.

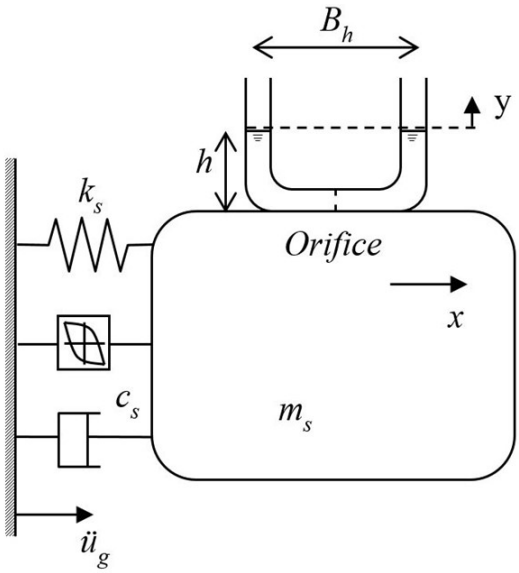

Figure 1*. Model of non-linear structure with TLCD.*

where c_s is the damping of the main system; k_s is the rigidity of the main system; m_s is the main mass of the system; B_h is the horizontal length of the tube; h is the height of the liquid column; $\ddot{u}_g$ is the acceleration of the ground; y is the displacement of the liquid within the column and x is the displacement of the main structure.

2.2. Equation of motion of the TLCD.

The equation of motion of a TLCD coupled to a single degree of freedom structure under a base acceleration $\ddot{u}_g$ is assessed as shown in Equation 1:

$$\rho A L_e \ddot{y} + \frac{1}{2}\rho A \xi |\dot{y}| \dot{y} + 2\rho g A y = -\rho A B_h \left(\ddot{x} + \ddot{u}_g \right) \tag{1}$$

where ρ is the density of the liquid; A is the area of the transversal section of the pipe; $L_e = 2h + B_h$, is the total length of the liquid column; g is the acceleration of gravity and ξ is the head loss coefficient.

The non-linear term of Equation 1 can be statistically linearized through the inclusion of an equivalent linear damping c_p as shown in Equation 2:

$$\rho A L_e \ddot{y} + \frac{1}{2}\rho A c_p \dot{y} + 2\rho g A y = -\rho A B_h \left(\ddot{x} + \ddot{u}_g \right) \tag{2}$$

where c_p, considering a zero mean Gaussian stationary process is shown in Equation 3:

$$c_p = \frac{\xi \sigma_{\dot{y}}}{\sqrt{2\pi}} \tag{3}$$

$\sigma_{\dot{y}}$ is the standard deviation of the velocity of the liquid.

Normalizing Equation 2 with regard to the liquid mass, Equation 4 is found:

$$\ddot{y} + \frac{2c_p}{L_e}\dot{y} + \frac{2g}{L_e} y + p\ddot{x} = -p\ddot{u}_g \tag{4}$$

where $p = B_h / L_e$. is the length ratio.

Besides, the frequency of the liquid is $\omega_l = \sqrt{2g / L_e}$; the frenquency of the system is $\omega_s = 2\pi / T_s$, where T_s corresponds to the period of the main system and $\gamma = \omega_l / \omega_s$ is the tuning ratio.

2.3 Equations of the movement of the main system with TLCD

The equation of motion of the main non-linear system with an added TLCD is shown in Equation 5:

$$\left(m_s+\rho AB_h+2\rho hA\right)\ddot{x}+c_s\dot{x}+\alpha_s k_s x+\left(1-\alpha_s\right)zF_y=-\left(m_s+\rho AB_h+2\rho hA\right)\ddot{u}_g-\rho AB_h\ddot{y} \tag{5}$$

where, F_y is the yielding force; $\Delta Y=F_y/k_s$ is the yielding displacement; α_s is the ratio between the post-yielding stiffnes, k_p and the initial elastic stiffnes k_0.

Moreover, z is the dimensionless hysteretic variable of the Bouc-Wen model, which satisfies the following first order differential equation (Equation 6):

$$\Delta Y\dot{z}+\dot{x}\left(\lambda-\left|z\right|^{\eta}\left(\beta+\gamma\,\mathrm{sgn}\left(z\right)\mathrm{sgn}\left(\dot{x}\right)\right)\right)=0 \tag{6}$$

with $\tilde{a}$ and $\hat{a}$ being dimensionless parameters which regulate the form of the hysteretic cycle, ë is the general scale factor and ç is the parameter which controls the softness of the transition between the linear and non-linear region.

The strength reduction factor R_u, is defined as shown in Equation 7:

$$R_u=\frac{f_{max}^{el}}{F_y} \tag{7}$$

where f_{max}^{el} corresponds to the maximum elastic force.

Substituting with $m_l=\rho AB_h+2\rho hA$ in Equation 5 and normalizing with regard to the mass, it has found Equation 8:

$$\left(1+\mu\right)\ddot{x}+2\xi_s\omega_s\dot{x}+\alpha_s\omega_s^2x+\frac{\left(1-\alpha_s\right)}{m_s}zF_y=-\left(1+\mu\right)\ddot{u}_g-\mu p\ddot{y} \tag{8}$$

where, $\mu=\rho AL_e/m_s$ is the mass ratio between the TLCD and the main system and $\hat{\imath}_s$ is the critical damping ratio of the main system.

The non-linear equation of the statistically linearized main movement of the system is shown in Equations 9, 10 and 11.

$$\Delta Y\dot{z}+k_{eq}z+c_{eq}\dot{x}=0 \tag{9}$$

$$k_{eq}=\sqrt{\frac{2}{\pi}}\beta\left[\sigma_{\dot{x}}+\frac{\gamma_{\dot{x}z}}{\sigma_z}\right] \tag{10}$$

$$c_{eq}=\sqrt{\frac{2}{\pi}}\beta\left[\sigma_z+\frac{\gamma_{\dot{x}z}}{\sigma_{\dot{x}}}\right]-1 \tag{11}$$

where $\gamma_{\dot{x}z}$ corresponds to the covariance of $\dot{x}$ and z, k_{eq} and c_{eq} are the equivalent damping and stiffnes, respectively, of the statistically linearized main system.

The equations, Equation 4, Equation 8 and Equation 9 can matricially be expressed as shown in Equation 12:

$$\begin{bmatrix} 1 & p & 0 \\ \mu p & (1+\mu) & 0 \\ 0 & 0 & 0 \end{bmatrix} \begin{Bmatrix} \ddot{y} \\ \ddot{x} \\ \ddot{z} \end{Bmatrix} +$$
$$\begin{bmatrix} 2c_p / L_e & 0 & 0 \\ 0 & 2\xi_s \omega_s & 0 \\ 0 & c_{eq} & \Delta Y \end{bmatrix} \begin{Bmatrix} \dot{y} \\ \dot{x} \\ \dot{z} \end{Bmatrix} +$$
$$\begin{bmatrix} 2g / L_e & 0 & 0 \\ 0 & \alpha\omega_s^2 & (1-\alpha) F_y / m_s \\ 0 & 0 & k_{eq} \end{bmatrix} \begin{Bmatrix} y \\ x \\ z \end{Bmatrix} = \begin{Bmatrix} -p \\ -(1+\mu) \\ 0 \end{Bmatrix} \ddot{u}_g \tag{12}$$

It is seen from Equation 12 that the mass associated to the hysteretic variable is null, which implies to express Equation 13 in terms of space of state, allowing assigning to the vector of state $\boldsymbol{q}$ the degrees of freedom related to the mass, by means of the submatrices $\boldsymbol{M}_1, \boldsymbol{C}_1, \boldsymbol{K}_1$ and $\boldsymbol{r}_1$. Then Equation 13 corresponds to the equation of state of the main system of two non-linear degrees of freedom with the TLCD added.

$$\dot{\boldsymbol{q}} = \boldsymbol{A}\boldsymbol{q} + \boldsymbol{B}_{\boldsymbol{u}} \ddot{u}_g \tag{13}$$

where, $\boldsymbol{q} = \{ y \quad x \quad \dot{y} \quad \dot{x} \quad z \}$ is the vector of state that includes the degrees of freedom of the system x, the TLCD y, and the hysteretic variable z.

Equation 14 shows the linearized matrix of the state for the whole system, and Equation 15 shows the influence matrix of state of the input, where the matrices $\boldsymbol{M}_1, \boldsymbol{C}_1, \boldsymbol{K}_1$ and $\boldsymbol{r}_1$ are submatrices from the mass matrix $\boldsymbol{M}$, the damping matrix $\boldsymbol{C}$, and the stiffness matrix $\boldsymbol{K}$ and from the influence vector $\boldsymbol{B}_{\boldsymbol{u}}$, respectively, related to the degree of freedom associated to mass and shown in Equation 16. On the other hand, $\boldsymbol{Z}_2, \boldsymbol{C}_2$ and $\boldsymbol{K}_2$ are the placement matrices of the hysteric variable z and of the equivalent damping c_{eq} of the statistical linearization of the Bouc-Wen equation and shown in Equation 17.

$$\boldsymbol{A} = \begin{bmatrix} 0_{2x2} & \boldsymbol{I}_{2x2} & 0_{2x1} \\ -\boldsymbol{M}_1^{-1}\boldsymbol{K}_1 & -\boldsymbol{M}_1^{-1}\boldsymbol{C}_1 & -\boldsymbol{M}_1^{-1}\boldsymbol{Z}_2 \\ 0_{1x2} & \boldsymbol{C}_2 & \dfrac{-k_{eq}}{\Delta Y} \end{bmatrix}. \tag{14}$$

$$\boldsymbol{B}_{\boldsymbol{u}} = \begin{bmatrix} 0_{2x1} \\ -\boldsymbol{M}_1^{-1}\boldsymbol{r}_1 \\ 0 \end{bmatrix} \tag{15}$$

$$\boldsymbol{M}_1 = \begin{bmatrix} 1 & p \\ \mu p & (1+\mu) \end{bmatrix} \quad \boldsymbol{C}_1 = \begin{bmatrix} 2c_p / L_e & 0 \\ 0 & 2\xi_s \omega_s \end{bmatrix} \quad \boldsymbol{K}_1 = \begin{bmatrix} 2g / L_e & 0 \\ 0 & \alpha\omega_s^2 \end{bmatrix} \tag{16}$$

$$\boldsymbol{Z}_2 = \begin{Bmatrix} 0 \\ \dfrac{(1-\alpha_s)}{m_s} F_y \end{Bmatrix} \quad \boldsymbol{C}_2 = \begin{Bmatrix} 0 & \dfrac{-c_{eq}}{\Delta Y} \end{Bmatrix} \quad \boldsymbol{r}_1 = \begin{Bmatrix} p \\ (1+\mu) \end{Bmatrix} \tag{17}$$

where $\boldsymbol{Z}_2$ is the influence matrix of the hysteric variable z in equation determined for the degrees of freedom not associated to mass and $\boldsymbol{C}_2$ and $\boldsymbol{K}_2$ are the placement matrices of the equivalent damping and equivalent stiffness, obtained from the statistical linearization of the Bouc-Wen related to the hysteric variable z also not associated to mass, as shown in Equation 17.

2.4 Calculation of the covariance matrix

The covariance matrix, V_q, is obtained from Equation 18:

$$\boldsymbol{V}_q = E\left\{\boldsymbol{q}(t)\boldsymbol{q}(t)^T\right\} = \frac{1}{2\pi}\int_{-\infty}^{\infty} \boldsymbol{H}_q(j\omega)\boldsymbol{S}_g(\omega)\boldsymbol{H}_q^*(j\omega)d\omega \tag{18}$$

where, $E\{\cdot\}$ = expected value of the process; $\boldsymbol{H}_q(j\omega)$ is defined as the response in frequency matrix which is obtained from Equation 19:

$$\mathbf{H_q}(j\omega) = \left[\mathbf{A} + j\omega\mathbf{I}\right]^{-1\prime} = \boldsymbol{\theta}\left[\boldsymbol{\lambda} + j\omega\mathbf{I}\right]^{-1}\boldsymbol{\theta}^{-1} \quad \boldsymbol{H}_q(j\omega) = \left[\boldsymbol{A} + j\omega\boldsymbol{I}\right]^{-1} = \boldsymbol{\theta}\left[\boldsymbol{\lambda} + j\omega\boldsymbol{I}\right]^{-1}\boldsymbol{\theta}^{-1} \tag{19}$$

where, $\boldsymbol{\lambda}$ is the eigenvalues matrix; $\boldsymbol{\theta}$ is the eigenvectors of $\boldsymbol{A}$; and $\boldsymbol{I}$ is the identity matrix of order five, as shown in Equation 20:

$$\boldsymbol{S}_g(\omega) = S_0 \frac{\omega_g^4 + 4\xi_g^2\omega_g^2\omega^2}{\left(\omega_g^2 - \omega^2\right) + 4\xi_g^2\omega_g^2\omega^2} \frac{\omega^4}{\left(\omega_f^2 - \omega^2\right) + 4\xi_f^2\omega_f^2\omega^2} \tag{20}$$

where S_0 is the white intensity of noise; $\grave{u}_g$ and $\hat{\imath}_g$, correspond respectively to the frequency and damping of the stratum of the soil; $\grave{u}_f$ and $\hat{\imath}_f$ are the frequency and damping, respectively, of the low frequencies filter.

Two random processes are considered to characterize the seismic frequencies content of the excitation, one of broad bandwidth (BBP) and one of narrow bandwidth (NBP). The first, was obtained from the calibration by minimum squares of the parameters of Equation 20 to the spectral power density of an artificial seismic event compatible with the design spectrum of NCh2745 for B site class; and the second, is derived from the power spectral density of the 1985 Mexico Earthquake. The parameters of both processes are found in Table 1.

Table 1. Parameters of the modified Kanai-Tajimi filter for the 2 random processes.

	S_0	$\grave{u}_g$ (rad/s)	$\hat{\imath}_g$	$\grave{u}_f$ (rad/s)	$\hat{\imath}_f$
NBP Process	1335.6	3.05	0.041	8.48	0.90
BBP Process	207.23	16.57	0.491	3.02	0.48

2.5 Hysteretic energy

The hysteretic energy has been used as a damage estimation index by many researchers (Lukkunaprasit & Wanitkorkul, 2001; Miranda, 2005; Pinkaew, Lukkunaprasit, & Chatupote, 2003; Sgobba & Marano, 2010; Wong & Johnson, 2009). As a result, in this research, the behavior of hysteretic energy dissipated by the main structure is studied as a damage estimation index.

The energy balance equation obtained from the equation of motion, of a non-linear structural model subjected to a seismic movement $\ddot{u}_g$ is shown in Equation 21:

$$e_k(t) + e_d(t) + e_h(t) + e_e(t) = e_I(t) \tag{21}$$

where, $e_k(t)$ is the kinetic energy; $e_d(t)$ is the energy dissipated by damping; $e_h(t)$ is the hysteretic energy, $e_e(t)$ the elastic energy; $e_I(t)$ is the seismic input's energy.

In particular, the term of the dissipated hysteretic energy can be calculated as shown in Equation 22:

$$e_h = \frac{E}{m} = (1-\alpha_s)\omega_s^2 \int_0^t z(\tau)\dot{x}(\tau)d\tau \tag{22}$$

This equation can be stochastically evaluated through the average value (Sgobba & Marano, 2010), as shown in Equation 23:

$$e_h = (1-\alpha_s)\omega_s^2 \int_0^T \gamma_{\dot{x}z}(\tau)d\tau = (1-\alpha_s)\omega_s^2 \gamma_{\dot{x}z} T \tag{23}$$

2.6 Optimization procedure

Two objective functions to minimize are proposed in this research. The first is the reduction of the main system's displacement standard deviation, criterion one (Cr1), as shown in Equation 24:

$$Minimize: J(\gamma,\xi) = Min(\sigma_x) \tag{24}$$

The second target function, corresponds to reducing the energy dissipated by the system, criterion two (Cr2), as shown in Equation 25:

$$Minimize: J(\gamma,\xi) = Min(e_h) \tag{25}$$

The two optimization criteria are subject to the restriction that the liquid's displacement has within the container, which is expressed in Equation 26:

$$h - c\sigma_y \geq 0 \tag{26}$$

Where, c=2.5, corresponds to the peak factor used in this study, and σ_y is the standard deviation of the vertical displacement.

3 RESULTS

According to the two aforementioned criteria, the influence of the mass ratio and the length ratio of the TLCD, the critical damping ratio of the main system, the resistance reduction factor, and the structural period, were analyzed over the optimal parameters of the device. The efficiency of the TLCD in controlling the response of the main system from the point of view of the displacement and the hysteretic energy was also analyzed. The analysis was made for the structure with the TLCD, considering two random processes as seismic excitation, one broad bandwidth (BBP) and the other narrow bandwidth (NBP), which are provided in Table 1.

3.1 Influence of the mass ratio on the optimal parameters of the TLCD

Figure 2 and Figure 3 respectively show the influence of the mass ratio of the TLCD on the optimal parameters of the TLCD obtained via the minimization of the standard deviation of the displacement of the main system (Cr1) (Figure 2), and of the minimization of the hysteretic energy of the structure (Cr2) (Figure 3), where row (a) corresponds to the analysis made with a random excitation of the broad bandwidth and row (b) with a narrow bandwidth process. The first column shows the ratio between the optimal frequency of the TLCD and the frequency of the main system, and the standardized linear equivalent frequency with regard to the frequency of the main system (LEF); in the second column, the optimal damping of the TLCD is provided; in the third and fourth columns, the reductions which the structure reaches thanks to the inclusion of an optimal TLCD are shown. The reductions correspond to the quotient between the standard displacement deviation of the system with TLCD with regard to the standard deviation without TLCD and the hysteretic energy dissipated by inelastic inclusion of the system with an optimal TLCD and the hysteretic energy of the system without TLCD, respectively. All the graphs of Figure 3 show the results for three periods, 2, 2.5 and 3 seconds, which present a range from least flexible structures to the most flexible ones.

In Figures 2 and 3, it is seen that the optimal tuning ratio of the TLCD in a BBP is insensitive to the mass ratio, and is higher the more flexible the structure is. On the other hand, as the structure becomes more flexible, the TLCD tends to tune with the linear equivalent frequency of the system without TLCD.

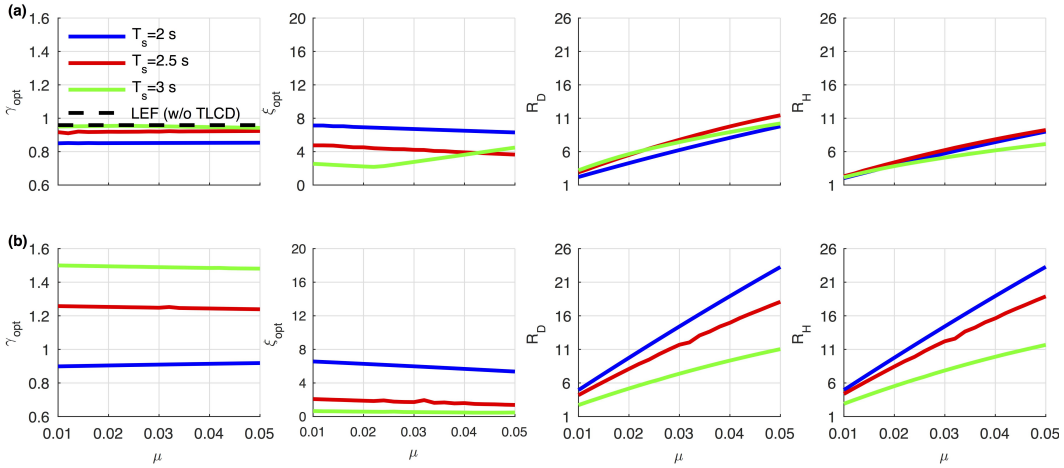

***Figure 2**. Optimal parameters with R_u=2, p=0.7, á$_s$=0.5 and î$_s$=0.05. (a) BBP; and (b) NBP. Criterion 1. LEF: linear equivalent frequency.*

The optimal head loss coefficient decreases linearly for less flexible structures, being higher in lower period structures; however, for more flexible structures, there is a change of slope. Besides, the efficiency of the TLCD increases as the mass ratio goes up; however, for more flexible structures there is a change in the efficiency starting from the mass ratio that changes the slope of the head loss coefficient. This is why, for lower mass ratios related to the change of slope, the TLCD is more effective from the point of view of the displacements in structures with a period higher. With regard to the hysteretic energy reduction, the efficiency of the TLCD is lower in more flexible structures.

It is also seen that in narrow bandwidth processes, as the structure becomes more flexible, the TLCD tends to tune with the predominant period of the input ($T_p = 2$ sec).

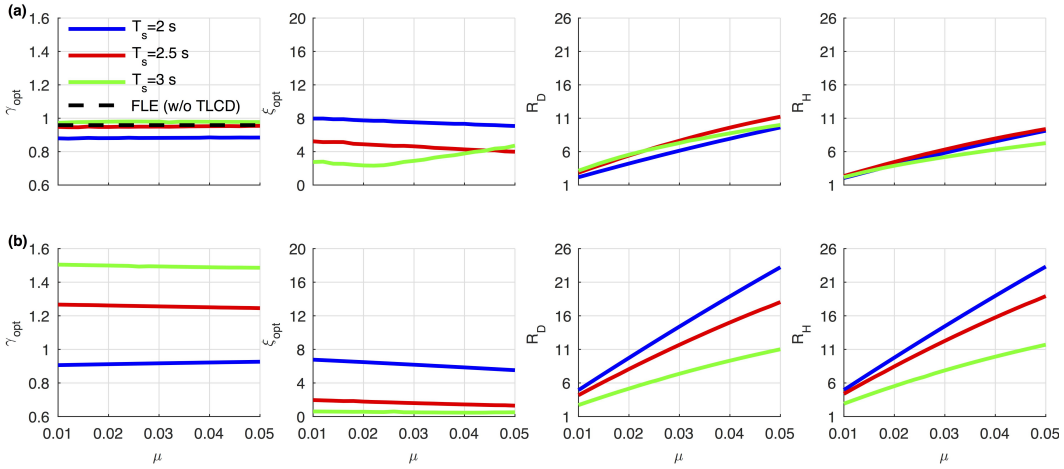

***Figure 3**. Optimal parameters with R_u=2, p=0.7, á$_s$=0.5 and î$_s$=0.05. (a) BBP; and (b) NBP. Criterion 2. LEF: linear equivalent frequency.*

It is also observed that the TLCD has similar efficiencies regarding the reduction of the displacement and the hysteretic energy.

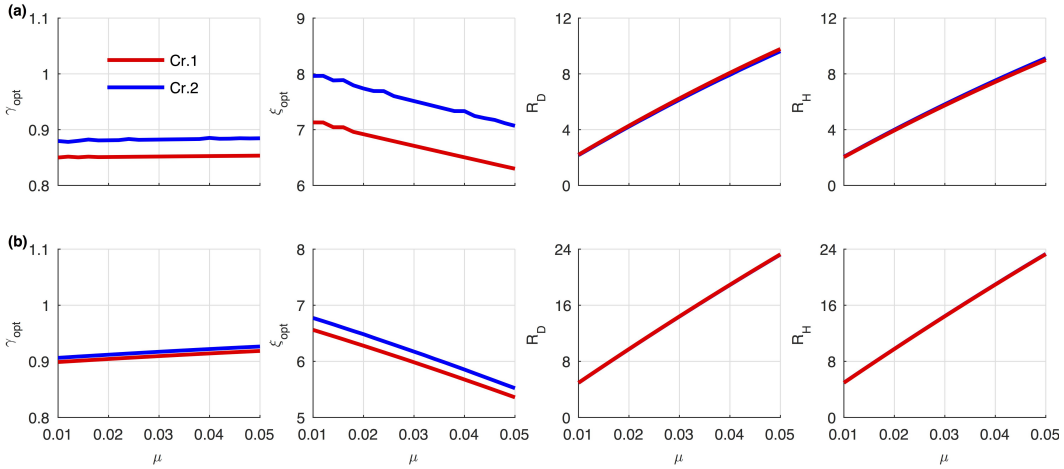

***Figure 4**. Optimal parameters with T_s= 2s R_u=2, p=0.7, á$_s$=0.5 and î$_s$=0.05. (a) BBP; and (b) NBP. Cr 1: Criterion 1. Cr 2: Criterion 2.*

The optimal head loss coefficient decreases as the mass ratio increases, and it is maximal when the period of structure coincides with the predominant period of the input. In addition, the efficiency of the TLCD increases as the mass ratio is higher, and such efficiency is maximal when the period of the structure coincides with the predominant period of the input, reaching the double of the reduction found in BBP.

From Figures 2 and 3, it is seen that the behavior of the optimal parameters of the TLCD and the reductions attained as not very sensitive to the optimization criterion used. This coincides with what was seen by Sgobba and Marano (Sgobba and Marano, 2010), in the analog study made on the tuned mass damper (TMD).

Figure 4 shows the optimal parameters for the same structure and for the two optimization criteria considered in the study (Cr1 and Cr2), for one broad bandwidth (BBP) and one narrow bandwidth (NBP) process.

It is seen that there are differences between the optimal parameters for both criteria, but on a very low scale, with this difference being greater in the case of BBP. In terms of the displacement and hysteretic energy reduction that the structure attains on incorporating an optimal TLCD, this is practically the same in both criteria.

3.2 Influence of the length ratio on the optimal parameters of the TLCD

Figures 5 and 6 show the optimal frequency ratio, optimal head loss ratio and reductions of the TLCD on the displacements and the hysteretic energy of the main system, for criteria 1 and 2 respectively. The distribution and the properties of the structure and the TLCD considered are analog to those of Figure 2 and 3.

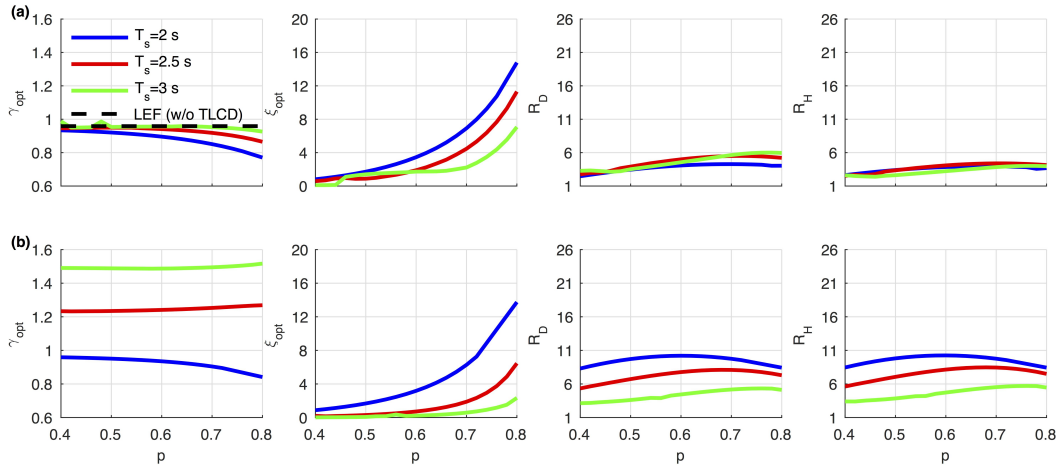

***Figure 5**. Optimal parameters with R_u =2, μ=0.02, α_s =0.5 and î$_s$ =0.05. (a) BBP; and (b) NBP. Criterion 1. LEF: linear equivalent frequency.*

From Figure 5, it is observed that for the BBP, the optimal tuning ratio of the TLCD tends to perfectly tune with the linear equivalent frequency of the structure without TLCD for low length ratios, decreasingly detuning as the length ratio of the TLCD increases, with this detuning being greater in less flexible structures.

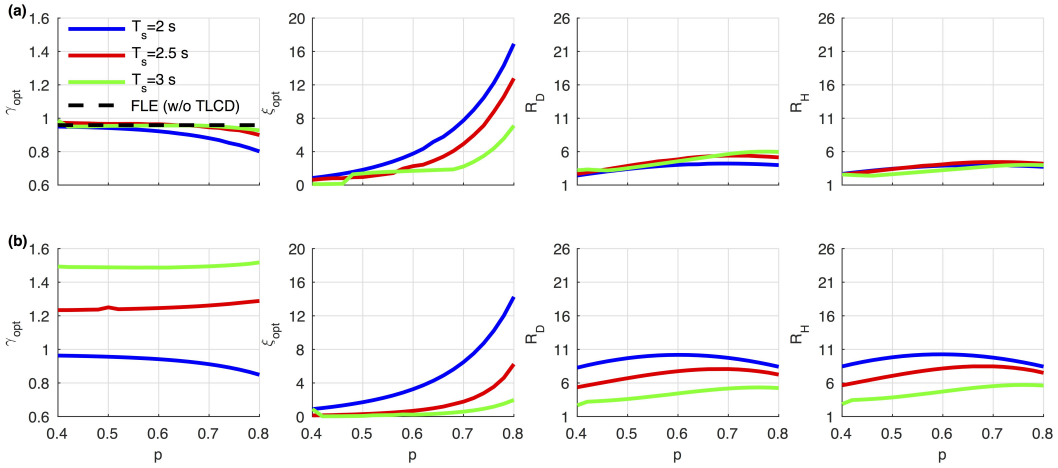

***Figure 6**. Optimal parameters with R_u =2, μ=0.02, α_s =0.5 and $\hat{\imath}_s$ =0.05. (a) BBP; and (b) NBP. Criterion 2. LEF: linear equivalent frequency.*

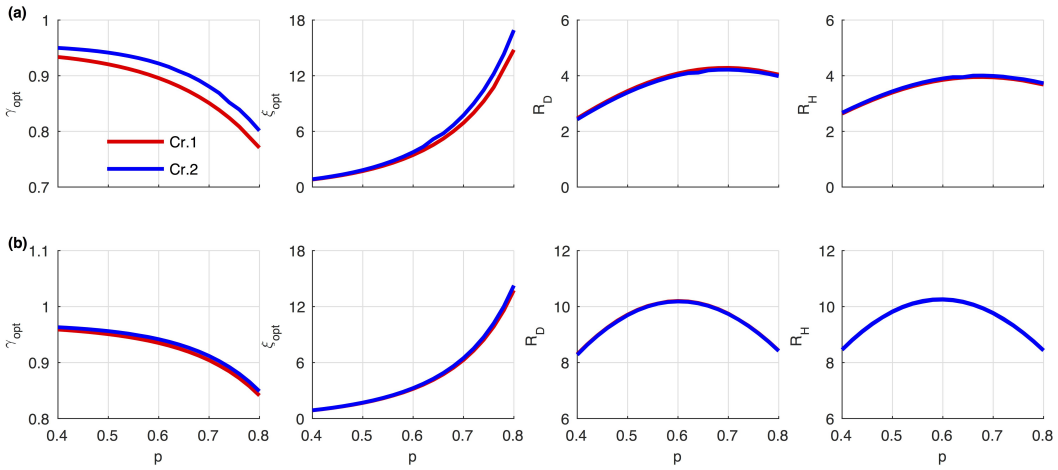

***Figura 7**. Optimal parameters with R_u =2, μ=0.02, α_s =0.5 y $\hat{\imath}_s$ =0.05. (a) BBP; y (b) NBP. Cr 1: Criterion 1. Cr 2: Criterion 2.*

On the other hand, it is seen that the optimal head loss coefficient increases as the length ratio increases, reaching higher values for less flexible structures. With regard to the displacement reductions of the main system and of the optimal hysteretic energy of the TLCD, the TLCD is seen to be not very efficient. In addition, it is seen that the efficiency of the TLCD is insensitive to the period of the main structure.

It is seen, from Figure 6, that in the case of a NBP, the TLCD is optimally tuned with the predominant period of the input (2 seconds), tuning which is more accurate the more flexible the period of the main structure is and the shorter the length ratio of the TLCD is; in addition, as the length ratio is greater the detuning is in the increasing direction for more flexible structures, and it is decreasing for more rigid structures. On the other hand, the head loss coefficient shows a similar behavior for both random processes; however, in NBP it reaches its highest value when the period of the structure coincides with the period of the predominant period of the excitation. It is seen, from the displacement and hysteretic energy reduction graphs, that the efficiency of the TLCD is greater when the period of the structure is closer to the predominant period of the random process.

Figure 7 shows, on a small scale, the behavior of the optimal parameters of the TLCD in terms of the length ratio for both optimization criteria, for a 2 second period structure. It is seen that there are differences between the optimal parameters obtained through the two criteria, but on a very small scale.

This difference is greater in the optimal tuning of the TLCD for a BBP and is imperceptible for NBP. As for the displacement and hysteretic reductions, there are no appreciable differences.

3.3 Influence of the damping ratio on the optimal parameters of the TLCD

Figure 8 and Figure 9 show the influence of the damping ratio on the behavior of the optimal head loss coefficient tuning ratio of the TLCD, and on the displacement and hysteretic energy reductions which is produced by the inclusion of an optimal TLCD on the structure. The distribution of the graphs and properties of the structure and of the TLCD, are the same as those of Figures 5 and 6.

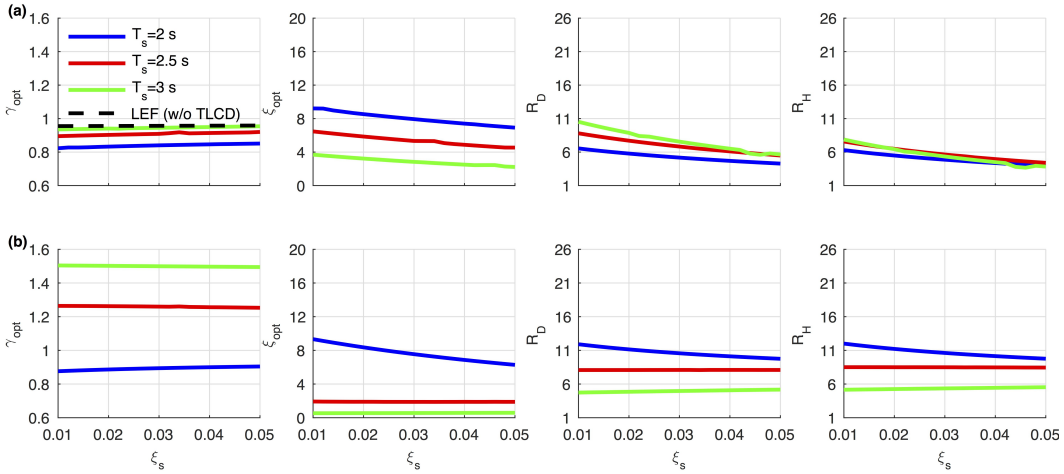

***Figure 8**. Optimal parameters with R_u=2, ì=0.02, á$_s$=0.5 and p =0. 7. (a) BBP; and (b) NBP. Criterion 1. LEF: linear equivalent frequency.*

It can be seen from Figures 8 and 9, that for broad bandwidth processes, the optimal tuning ratio of the TLCD is insensitive to the damping ratio of the structure, approaching the tuning more with the linear equivalent frequency of the system without TLCD as the structure becomes more flexible. As for the optimal head loss coefficient of the TLCD, it is seen that this decreases as the damping of the structure increases, being higher in shorter period structures. On the other hand, the efficiency of the TLCD decreases as the damping ratio of the structure is greater, and it is greater in more flexible structures, especially in the control of the displacement of the main system.

For a NBP, the optimal tuning ratio of the TLCD is insensitive to the damping ratio of the structure, finding that as the system becomes more flexible, the TLCD is tuned with the predominant frequency of the excitation (ð). In regard to the optimal head loss coefficient, it is observed that it is greater as the period of the structure is getting closer to predominant period of the excitation.

On the other hand, it is seen that the efficiency decreases as the damping of the main system increases, and is greater when the period of the structure coincides with the period of the excitation, being insensitive to damping in the other periods analyzed. It is also observed that the efficiency is greater for NBP.

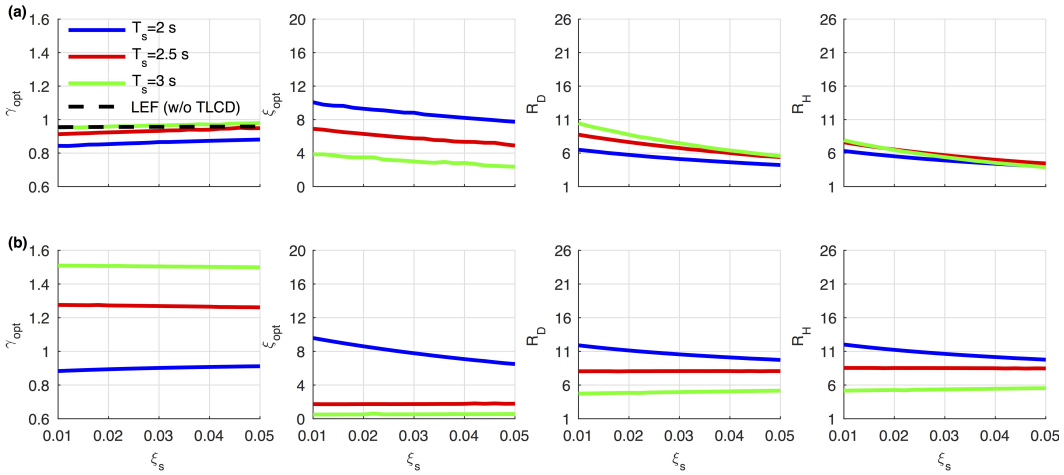

***Figure 9**. Optimal parameters with R_u=2, ì=0.02, á$_s$=0.5 and p =0. 7. (a) BBP; and (b) NBP. Criterion 2. LEF: linear equivalent frequency.*

Figure 10 shows, on a smaller scale, the behavior of the optimal parameters of the TLCD in terms of the length ratio for both optimization criteria, and just like in Figure 7 for a 2 second period structure.

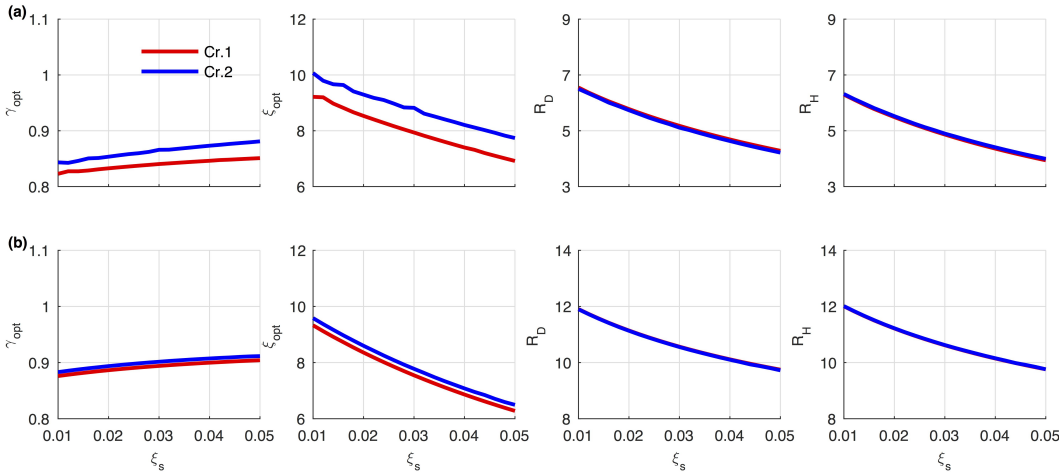

***Figure 10**. Optimal parameters with R_u=2, ì=0.02, á$_s$=0.5 y p =0. 7 (a) BBP; y (b) NBP. Cr 1: Criterion 1. Cr 2: Criterion 2.*

Differences are seen in the optimal parameters for both criteria, but on a very small scale, finding greater differences in the tuning ratio and the optimal head loss coefficient in broad bandwidth processes. The reductions obtained for both criteria do not depend on the optimization functional used.

3.4 Influence of the Reduction Factor on the optimal parameters of the TLCD

Figures 11 and 12 show the optimal parameters of the TLCD in terms of the Reduction Factor of the structure.

The setup of the graphs, structure properties, TLCD and the characteristics of the excitation are analog to those of Figures 8 and 9.

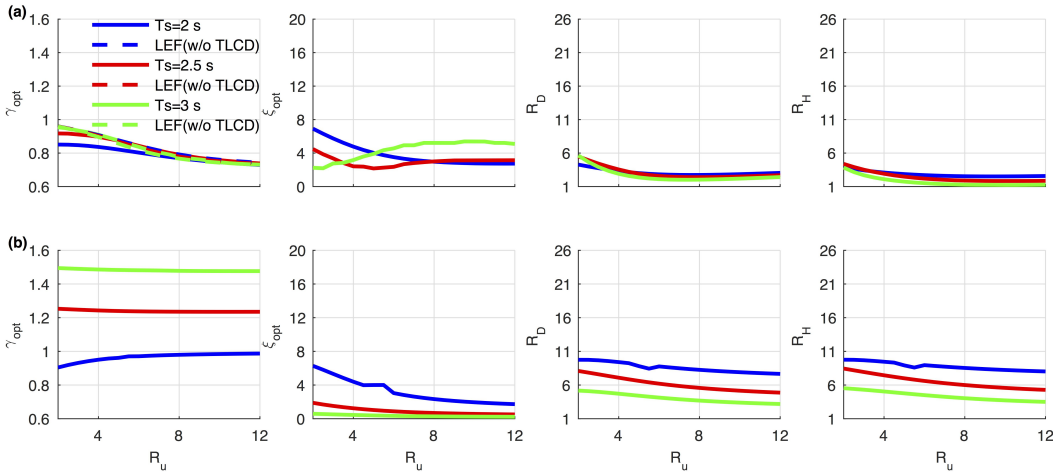

Figure 11. *Optimal parameters with îs=0.05, ì=0.02, ás=0.5 and p =0. 7. (a) BBP and (b) NBP. Criterion 1. LEF: linear equivalent frequency.*

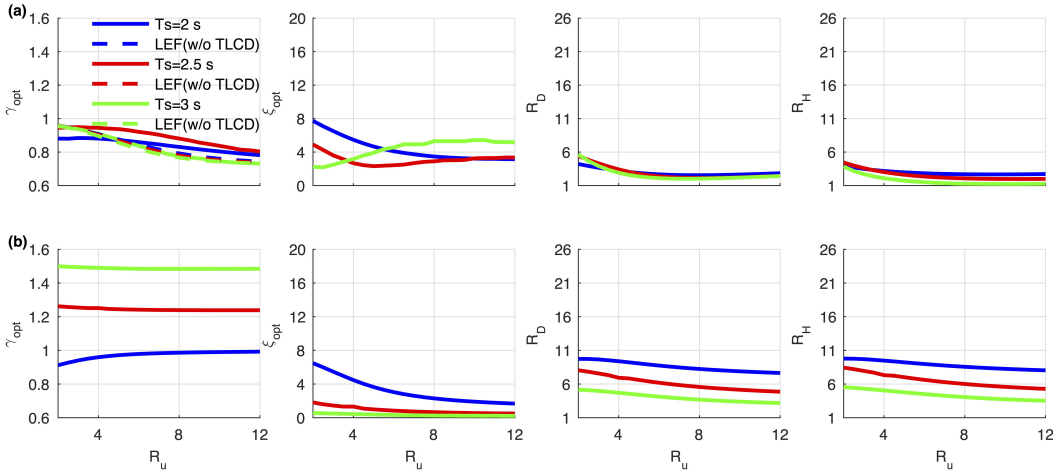

Figure 12*. Optimal parameters with îs=0.05, ì=0.02, ás=0.5 and p =0. 7. (a) BBP and (b) NBP. Criterion 2. LEF: linear equivalent frequency.*

Figure 11 shows that for BBP, the tuning ratio tends to tune with the linear equivalent frequency of the system without TLCD. On the other hand, as the structure becomes more non-linear, it is detuned with regard to the frequency of the main system. This behavior can be expected, as there is a degradation of the associated stiffnes when entering the non-linear range. It is also seen, that when the structure has had a slight incursion into the non-linear range, the optimal tuning ratio of the TLCD is lower for less flexible structures and as the non-linearity increases, the tuning ratio is the same for all the structures, being insensitive to the period of the structure and coinciding with the linear equivalent frequency of the main system without TLCD.

Figure 12 shows that for BBP, the optimal tuning ratio of the TLCD is detuned with regard to the frequency of the main system as the structure enters further into the non-linear range, but is not tuned with the linear equivalent frequency of the system without TLCD. This behavior is seen in criterion 1 (Figure 11). It is also seen, that the tuning ratio of the more rigid structures has a lower magnitude.

In addition, it is observed from Figures 11 and 12 that in BBP the value of the optimum head loss coefficient is dependent on a point of inflection that occurs for lower degrees of inelastic incursion into more flexible structures, increasing its value after this one. On the other hand, the reductions that an optimal TLCD produces in a structure, which has entered the non-linear range, are insensitive to the flexibility of the structure.

While, it is also seen in Figure 11 and Figure 12, that in the case of a NBP, the TLCD tends to be tuned to the predominant period of the input ($T_i = 2$ sec), tuning which rises as the system enters further into the non-linear range. It is also seen that the head loss coefficient decreases as the system enters further into the non-linear range, and has a lower magnitude in more rigid structures. On the other hand, the TLCD is more efficient for narrow

bandwidth excitations, producing greater reductions, both in the displacement and hysteretic energy in more flexible structures.

Figure 13 shows, on a smaller scale, the behavior of the optimal parameters of the TLCD in terms of the reduction factor for both optimization criteria and, just like in Figure 10, for a 2 second structure perio

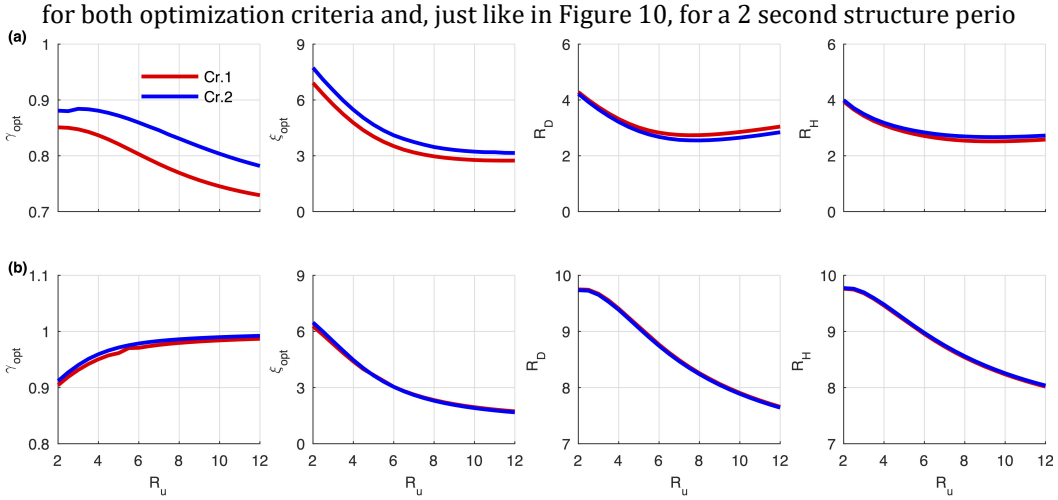

***Figure 13**. Optimal parameters with îs=0.05, ì=0.02, ás=0.5 and p =0. 7 subject to one process: (a) BBP; and (b) NBP. . Cr 1: Criterion 1. Cr 2: Criterion 2.*

It is seen that there are differences between the optimal parameters in terms of the reduction factor obtained for both criteria, and that the differences are greater in the tuning ratio and optimal head loss coefficient for a BBP. In the other cases, the differences between the reductions obtained through both optimization criteria are negligible.

3.5 Main structure period influence on the optimal parameters of the TLCD

3.5.1 Regarding the mass ratio

Figures 14 and 15 show the optimal parameters of the TLCD in terms of the period of the structure. These are analyzed for the three mass ratios (μ= 0.1, 0.2 and 0.5). The setup of the graphs, properties of the structure, TLCD and the characteristics of the excitation are analog to those of Figures 11 and 12.

It is seen that for a random excitation of the broad bandwidth, the optimal tuning ratio of the TLCD converges, towards high periods, to the linear equivalent frequency of the structure without TLCD. As for the optimal head loss coefficient of the TLCD, it is seen that this decreases the more flexible the structure is and is slightly lower as the mass ratio increases. In turn, for the efficiency of the TLCD, it is greater for a TLCD with greater mass ratios and it is practically unsensitive to the period of the structure.

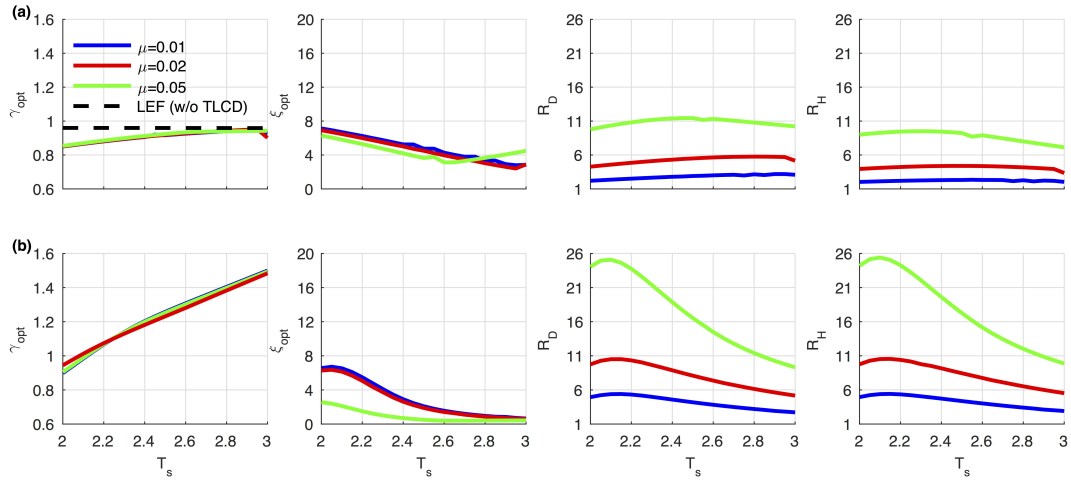

***Figure 14**. Optimal parameters with îs =0.05, Ru=2, ás=0.5 and p=0.7 (a) BBP and (b) NBP. Criterion 1. LEF: linear equivalent frequency.*

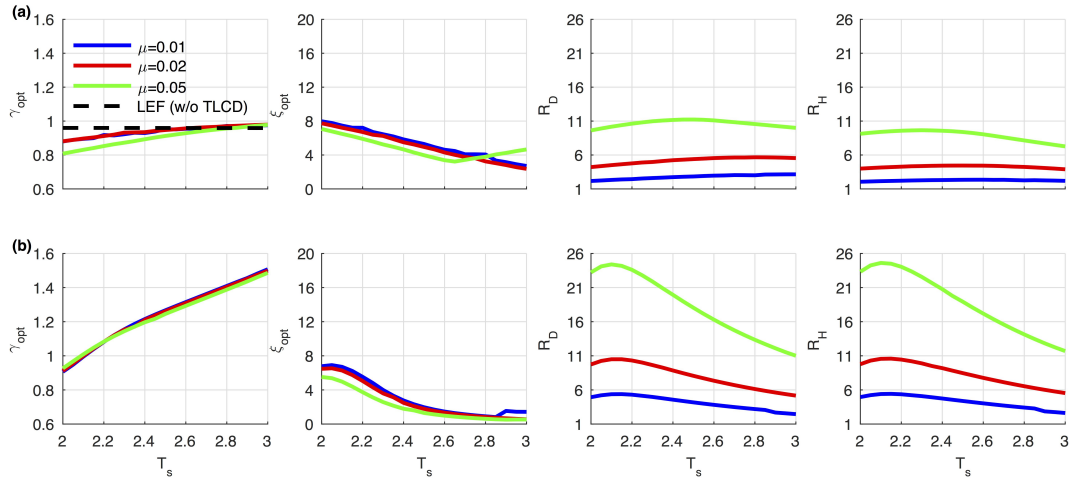

***Figure 15**. Optimal parameters with îs =0.05, Ru=2, ás=0.5 and p=0.7 (a) BBP and (b) NBP. Criterion 2. LEF: linear equivalent frequency.*

On the other hand, it is seen that for NBP (Figure 15 y 16), the tuning ratio of the TLCD increases linearly with a slope of 45° degrees, as it tunes with the predominant frequency of the excitation (ð) for all period values of the main structure and; therefore, is insensitive to the mass ratio of the structure.

It is seen that the optimal head loss coefficient is practically insensitive to the mass ratio of the TLCD, when this is small, adopting lower values for greater mass ratios.

In Figure 14 and 15, it can be seen that the displacement and hysteretic energy reductions, that the TLCD produces in a non-linear structures, are approximately the same in both cases, and are higher for higher mass ratios, being higher in NBP and reaching a maximum for periods close to the predominant period of the seismic input.

Figure 16 shows, on a smaller scale, the behavior of the TLCD's optimal parameters in terms of the structure's period for both optimization criteria, for a mass ratio of 0.05.

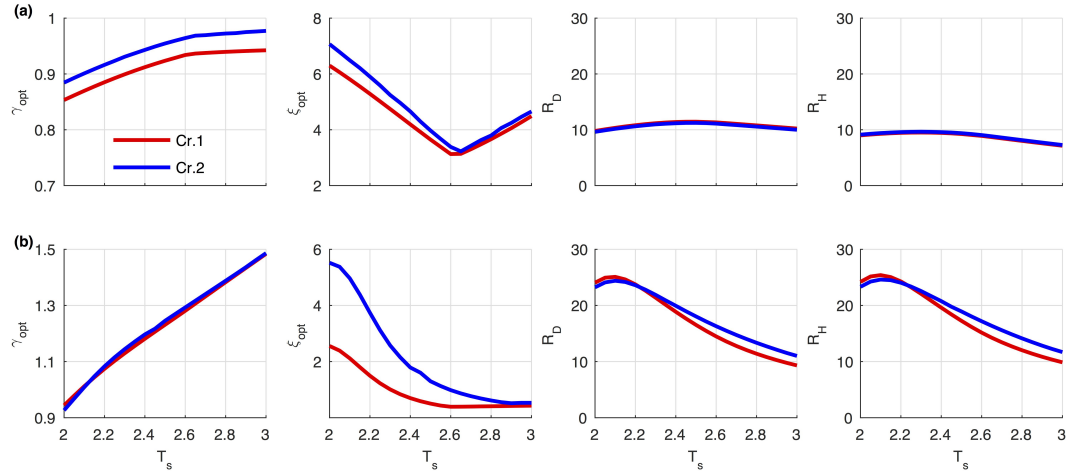

***Figura 16**. Parámetros óptimos con îs =0.05, p=0.7, ì=0.05, ás=0.5 y Ru=2 (a) BBP y (b) NBP. Cr 1: Criterion 1. Cr 2: Criterion 2.*

It is seen that for BBP, there are appreciable differences in the optimal tuning ratio obtained for both criteria for all the range of periods analyzed. On the other hand, the optimal head loss coefficient of the TLCD obtained for both criteria shows a difference, on a small scale, for low periods. In turn, for the efficiency of the TLCD in terms of displacement and damage, a dependence of the criterion considered in the optimization is not seen.

In NBP, both criteria lead to the same optimal tuning ratio, but an appreciable difference is seen in the optimal head loss coefficient in more flexible structures. With regard to the displacement and hysteretic energy reductions, appreciable differences are observed in structures with higher periods.

3.5.2 Regarding the length ratio

Figures 17 and 18 show the influence of the period of the main structure in the optimal parameters of the TLCD, for three length ratios of the TLCD (p=0.6, 0.7 and 0.8). Once again, the distribution of the properties of the structure, the TLCD and the type of excitation are the same as in Figures 14 and 15.

Se observa it is seen that in a random BBP, the optimal tuning ratio of the TLCD converges for high periods of the structure, to the linear equivalent frequency of the structure without TLCD. With regard to the influence of the length ratio, it is seen that the tuning ratio is higher for lower length ratios, and is insensitive to this when the structure is more flexible. On the other hand, the optimal head loss coefficient is higher for higher length ratios, and decreases in regard to the higher flexibility of the structure. In turn, for the efficiency of the TLCD in the control of the displacement, and hysteretic energy of the main system, it is independent of the length ratio of the TLCD. While, it is seen that for NBP the tuning ratio of the TLCD increases linearly with a slope of 45°, as the tuning ratio of the TLCD is tuned with the predominant frequency of the excitation (2 seconds), and it is insensitive to the value of the length ratio.

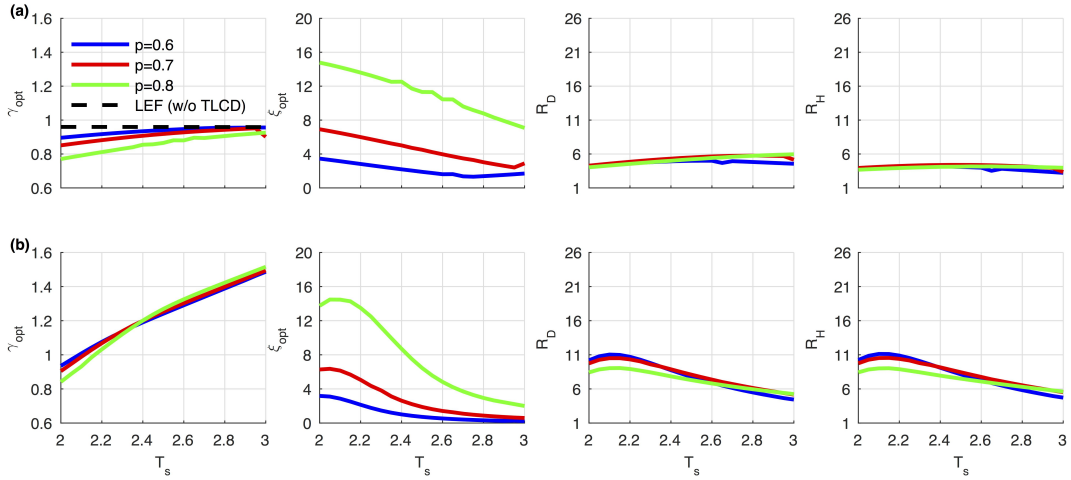

***Figure 17**. Optimal parameters with î_s =0.05, p=0.7, ì=0.02, á_s=0.5 and R_u=2 (a) BBP and (b) NBP. Criterion 1. LEF: linear equivalent frequency.*

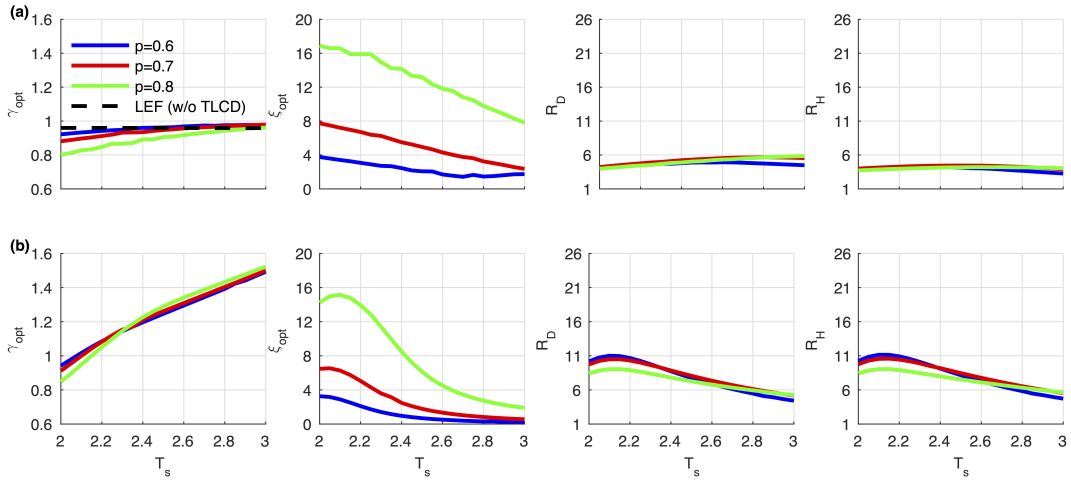

***Figure 18**. Optimal parameters with î_s =0.05, p=0.7, ì=0.02, á_s=0.5 and R_u=2 (a) BBP and (b) NBP. Criterion 2. LEF: linear equivalent frequency.*

On the other hand, the optimal head loss coefficient is sensitive to the value of the length ratio, adopting higher values the higher the length ratio is, reaching a maximum for periods close to the predominant period of the excitation. While, in Figures 17 and 18, it is seen that the efficiency of the TLCD is independent of the length ratio of the TLCD in BBP, and it varies slightly with this parameter in NBP, resulting in a smaller reduction for longer length ratios of the TLCD. Greater reductions are also observed for this random process.

Figure 19 shows, on a smaller scale, the behavior of the optimal parameters of the TLCD in terms of the period of the structure for both optimization criteria, for a length ratio of 0.6. Practically no differences are seen in the values of the optimal parameters obtained for both criteria, with the exception of the optimal tuning ratio of the TLCD and optimum head loss coefficient for random broad bandwidth processes.

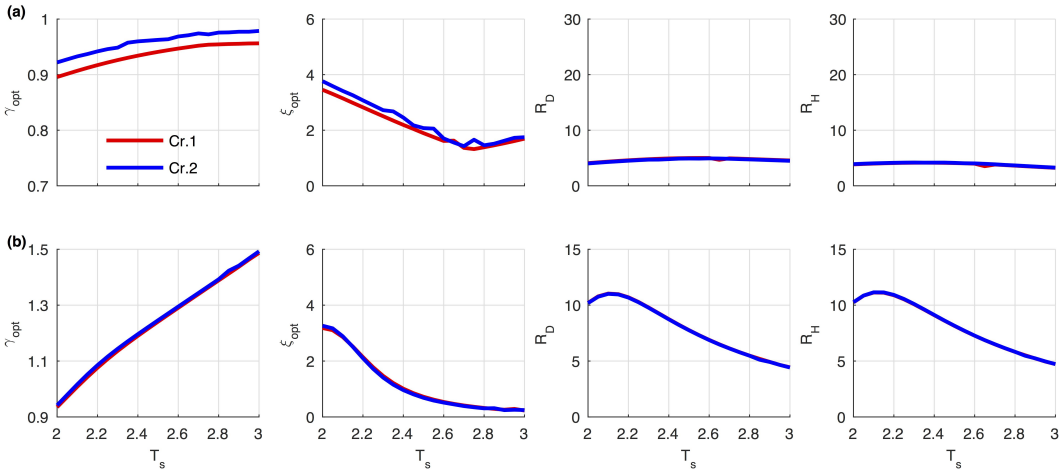

Figure 19*. Optimal parameters with î$_s$ =0.05, R$_u$=2, ì=0.02, á$_s$=0.5 and p=0.6 (a) BBP and (b) NBP. Cr 1: Criterion 1. Cr 2: Criterion 2.*

On the other hand, it is seen that for reductions both of the displacement and damage of the main system do not depend on the optimization criterion used.

4 CONCLUSIONS

From the research conducted, it is concluded that the optimal tuning ratio of the TLCD is insensitive to the mass ratio and to the damping ratio of the main system. In addition, the head loss coefficient is greater in less flexible structures.

On the other hand, the TLCD tends to optimally tune to the equivalent linear frequency, as the structure is more flexible, when it is subjected to a random process of broad bandwidth (BBP). In the case of a random process of narrow bandwidth (NBP), it is tuned to the predominant period of excitation. When the structure enters the non-linear range, the optimal frequency of the TLCD is detuned with respect to the initial frequency of the structure, when the random process is BBP and when the process of NBP is independent of the degree of non-linearity of the structure.

It is also concluded that the optimal head loss coefficient is greater in less flexible structures, and when the excitation is a BBP it decreases as the damping of the main system of the structure is greater, and it increases when the coefficient of loss of optimal load is greater. On the other side, as the structure enters more in the non-linear range, the optimal head loss coefficient decreases to a point of slope change that occurs for a lower degree of inelastic incursion as the structure is more flexible.

The TLCD is more efficient, both in displacement control and damage reduction, when its mass ratio is higher, being higher in NBP, reaching its maximum efficiency when it is tuned to the predominant frequency of the input.

In general, there is no appreciable difference between the values of the optimal parameters and reductions achieved, both in displacement and hysteretic energy obtained with each optimization criterion, being this result coinciding with those found by Sgobba and Marano (2010) for the behavior of the TMD.

5 ACKNOWLEDGEMENTS

This research has been financed by the Universidad del Bío-Bío through the DIUBB Research Project 132714 3/R. The authors thank the review of the manuscript provided by Mr. Franco Benedetti, Dr. Eric Forcael from the Civil and Environmental Engineerig Department of the University of Bio-Bio. His helpful comments are deeply appreciated.

References

Balendra, T., Wang, C.M. & Cheong, H.F. (1995). Effectiveness of tuned liquid column dampers for vibration control of towers. Engineering Structures, 17(9), pp.668–675.

Battista, R. C., Carvalho, E. M. L., Souza R de A. (2008). Hybrid fluid-dynamic control devices to attenuate slender strucures oscillations. Engineering Structures, 30, pp.3513-3522.

Bigdeli, Y. & Kim, D. (2015). Response control of irregular structures using structure-TLCD coupled system under seismic excitations. ASCE Journal of Civil Engineering, 19(3), pp.672–681

Cammelli, S. & Li, Y.F. (2016). Experimental and numerical investigation of a large tuned liquid column damper. Proceeding of the Institution of Civil Engineers – Structures and Buildings, 169(8), pp.1–8.

Chakraborty, S., Debbarma, R. & Marano, G.C. (2012). Performance of tuned liquid column dampers considering maximum liquid motion in seismic vibration control of structures. Journal of Sound and Vibration, 331(7), pp.1519–1531.

Di Matteo A., Lo Iacono F., Navarra G. & Pirrotta A. (2015). Innovative modeling of Tuned Liquid Column Damper motion. Communications in Nonlinear Science and Numerical Simula-tion, 23(1–3), pp.229–244

Esteva, L., and Ruiz, S. E. (1997). "Discussion on 'Stochastic seismic performance evaluation of tuned liquid column dampers'." Earthquake Eng. Struct. Dyn., 26, 875–876.

Gao, H., Kwok, K.C.S. & Samali, B. (1997). Optimization of tuned liquid column dampers. Engineering Structures, 19(6), pp.476–486.

Gao, H., Kwok, K.S.C. & Samali, B. (1999). Characteristics of multiple tuned liquid column dampers in suppressing structural vibration. Engineering Structures, 21(4), pp.316–331.

Ghosh, A. & Basu, B. (2004). Seismic vibration control of short period structures using the liquid column damper. Engineering Structures, 26(13), pp.1905–1913.

Ghosh, A. & Basu, B. (2008). Seismic Vibration Control of Nonlinear Structures Using the Liquid Column Damper. Journal of Structural Engineering, 134(1), pp.146–153.

Lee, S.K., Lee, H.R. and Min, K.W. (2010), "Experimental verification on nonlinear dynamic characteristic of a tuned liquid column damper subjected to various excitation amplitudes", Struct. Des. Tall Spec. Build., 21, 374-388

Lukkunaprasit, P., & Wanitkorkul, A. (2001). Inelastic buildings with tuned mass dampers under moderate ground motions from distant earthquakes. Earthquake Engineering and Structural Dynamics, 30(4), 537–551.

Miranda, J. C. (2005). On tuned mass dampers for reducing the seismic response of structures. Earthquake Engineering and Structural Dynamics, 34(7), 847–865.

Pinkaew, T., Lukkunaprasit, P., & Chatupote, P. (2003). Seismic effectiveness of tuned mass dampers for damage reduction of structures. Engineering Structures, 25(1), 39–46.

Rozas, L., Boroschek, R., Tamburrino, A.,& Rojas. M. (2016). A Bidirectional tuned liquid columnd damper for reducing seismic response of building. Struct. Control Monit., 23, pp, 21-640

Sadek, F., Mohraz, B. & Lew, H.S. (1998). Single- and multiple-tuned liquid column dampers for seismic applications. Earthquake Engineering & Structural Dynamics, 27(September 1997), pp.439–463.

Sakai, F., Takaeda, S. (1989), "Tuned liquid column damper- New type device for supression of building vibrations", Proc., Int. Conf. on High Rise Build, Nanjing, China, 926-931

Sgobba, M. and Marano, G.C. (2010), "Optimum design of linear tuned mass dampers for structures with nonlinear behavior", Mech. Syst. Sign. Proc., 24(6), 1739-1755.

Shum, K.M. (2009). Closed form optimal solution of a tuned liquid column damper for suppressing harmonic vibration of structures. Engineering Structures, 31(1), pp.84–92.

Souza, R.A.(2003). Active/passive control of oscillations of slender structures by means of fluid-dynamical devices, PfD Thesis COPPE/Federal University of Rio de Janeiro.

Won, A.Y.J., Pires, J.A. & Haroun, M.A. (1996). Performance assessment of tuned liquid column dampers under random seismic loading. International Journal of Non-Linear Mechanics, 32(4), pp.745–758.

Wong, K. K. F., & Johnson, J. (2009). Seismic Energy Dissipation of Inelastic Structures with Multiple Tuned Mass Dampers. Journal Engineering Mechanics, 135(4), 265–275.

Xu, Y.L., Kwok, K.C.S. & Samali, B. (1992). The effect of tuned mass dampers and liquid dampers on cross-wind response of tall/slender structures. Journal of Wind Engineering and Industrial Aerodynamics, 40(1), pp.33–54.

Yalla S.K. & Kareem A. (2000). Optimum absorber parameters for tuned liquid column dampers. Journal of Structural Engineering,126(8): 906–915.

Zeng, X., Yu, Y., Zhang, L., Liu, Q. & Wu, H. (2015). A new energy-absorbing device for motion suppression in deep-sea floating platforms. Energies, 8(1), pp.111–132.